Electronic Supplementary Information

Enhanced Electrochemical Performance of $LiMn_2O_4$ Cathode with a $Li_{0.34}La_{0.51}TiO_3$-Coated Layer

Sijiang Hu[a,c], Yu Li[b], Feiyan Lai[b], Xiaohui Zhang[b], Qingyu Li[b], Youguo Huang[b], Ximing Yuan[a,*], Jianjun Chen[d], Hongqiang Wang[b,c,*]

[a]School of Materials Science and Chemistry, China University of Geosciences, Wuhan 430074, PR China

[b]Guangxi Key Laboratory of Low Carbon Energy Materials, School of Chemistry and and Pharmaceutical Sciences, Guangxi Normal University, Guilin 541004, PR China

[c]Hubei Key Laboratory for Processing and Application of Catalytic Materials, College of Chemical Engineering, Huanggang Normal University, Huanggang 438000, PR China

[d]Research Institute of Tsinghua University in Shenzhen, Shenzhen 518057, P.R. China

Corresponding author's information:

Email address: whq74@mailbox.gxnu.edu.cn (H Wang), xmyuan@foxmail.com (X. Yuan)

Fax number:+86 773 5854077

The SEM images of single-phase LLTO is present in Fig. S1. It is found that LLTO is uniformly distributed with various pore size. We consider that this network porous structure is benefit to the following coating process.

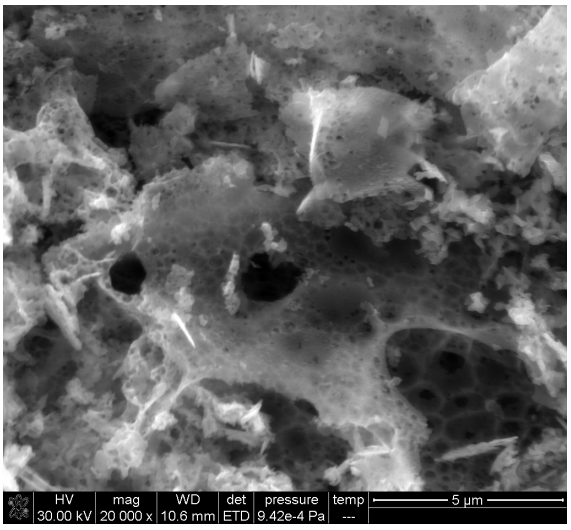

Fig. S1. SEM images of single-phase perovskite LLTO.

As shown in Table S1, change of lattice parameter can be neglected. The results indicate all samples have typical spinel structure.

Table S1. Lattice parameters of $LiMn_2O_4$ before and after LLTO surface coating obtained from the XRD patterns.

Sample	LLT0	LLT01	LLT03	LLT05
Lattice parameter (Å)	8.2436	8.2457	8.2449	8.2447

As displayed Fig. S2, the average diameters of LMO and LLTO are 7.61 and 12.98 μm. After ball milling process, particle size of the precursors are smaller than that of LMO and LLTO. All as-prepared samples show slight increased particle size after heat treatment.

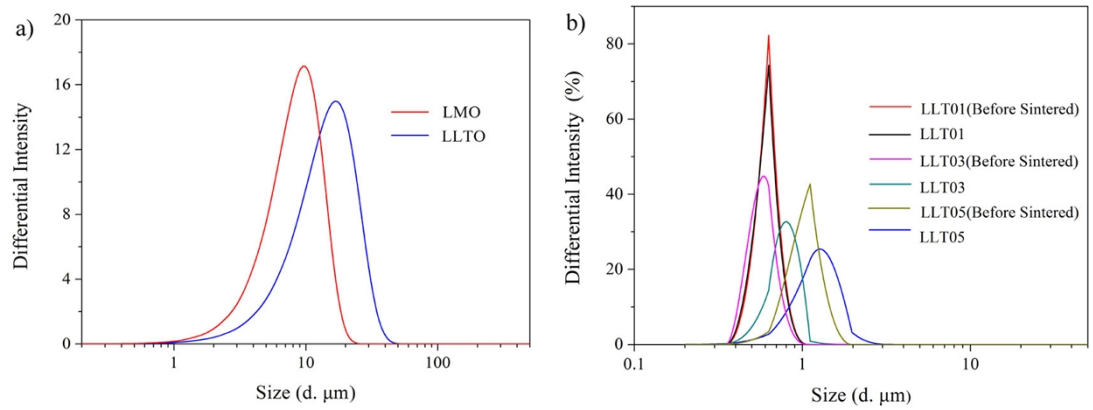

Fig. S2 Particle size distributions of LLTO and pristine LMO (a), before and after sintered LLT01, LLT03 and LLT05.

Fig. S3 compares discharge curves of LLT03 and LLT05 with 1, 50, 100, 200 cycles at 25 °C . It is seen from Fig. S3 that the discharge capacity of LLT05 suffers fast fading, though it exhibits a higher initial discharge capacity. As for LLT03, the capacities degrade slower with repeated cycling. The initial discharge capacity monotonically decreases with increasing coating content since LLTO is an inactive material.

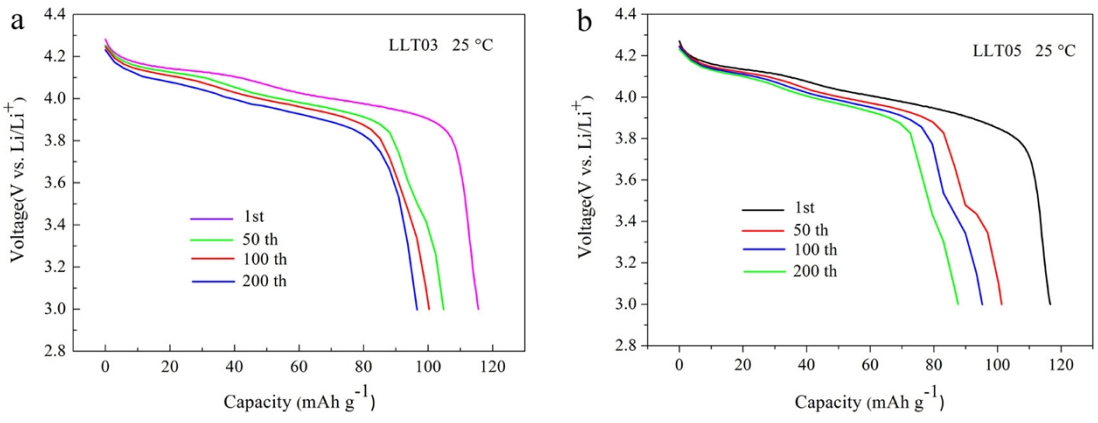

Fig. S3. The initial, 50th, 100th and 200th discharge curves of LLT03 (a) and LLT05 (b) cycled at

1 C at room temperature.

Fig. S4 shows the three-dimensional Nyquist plots of LLT0 and LLT01 for the initial discharge-charge cycle.

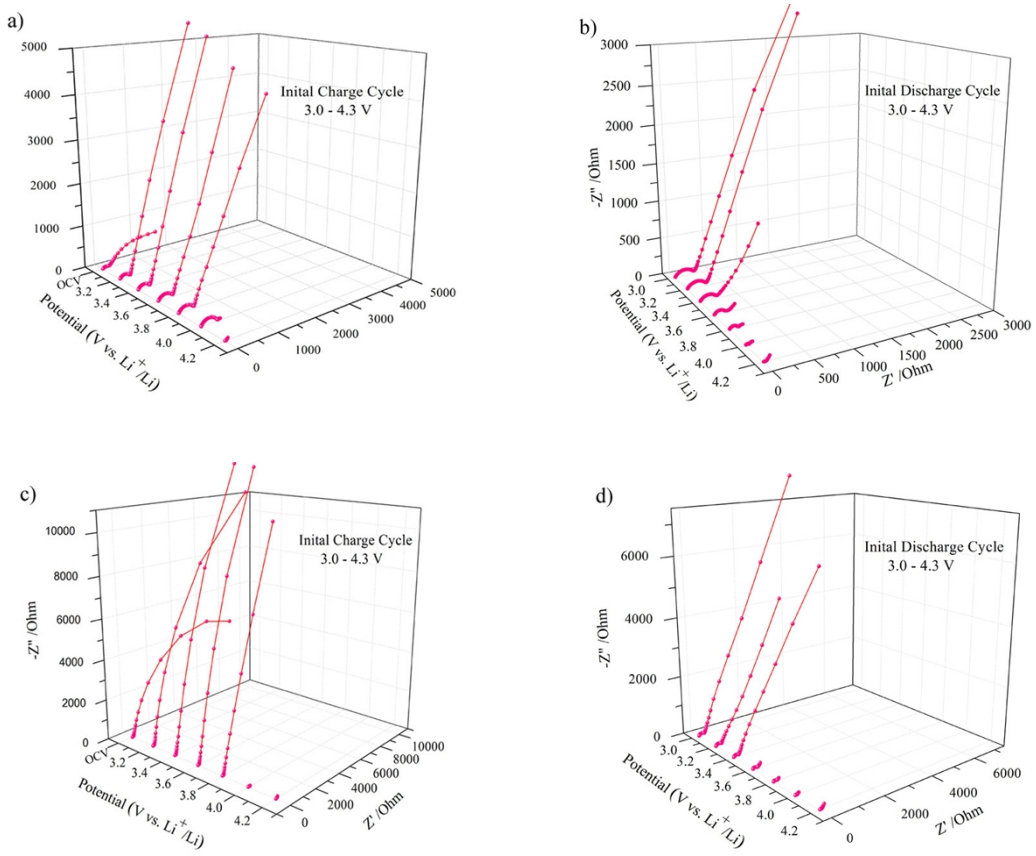

Fig. S4. Three-dimensional Nyquist plots for LLT0 (a) initial charge cycle (3.2-4.2 V), (b) initial discharge cycle (4.2-3.0 V) and LLT01 (c) initial charge cycle (3.2-4.2 V), (d) initial discharge cycle (4.2-3.0 V).

Fitting values for LLT0 and LLT01 during initial discharge-charge cycle are present in Table S2. The diffusion coefficient of Li ions was calculated by using the following equation [1-3]:

$$D_{Li+} = R^2T^2(2A^2n^4F^4C^2\sigma^2)^{-1}$$

Herein, R is the gas constant, T is the absolute temperature, A is the surface area of the cathode, n is the number of electrons per molecule during oxidization, F is the Faraday constant, C is the concentration of Li^+, σ is estimated from the gradient of a plot of -Z″ *vs*. $\omega^{-1/2}$.

Table S2. Fitting values for LLT0 and LLT01 during initial Discharge-Charge Cycle.

	R_s/Ω	$CPE_{sf}/\mu F$	R_{sf}/Ω	$CPE_{dl}/\mu F$	R_{ct}/Ω	D_{Li+} / cm^2s^{-1} ($\times 10^{-11}$)
LLT0 1st charge cycle						
3.0 (OCV)	11.16	—	—	0.68	110.8	1.75
3.2	9.25	—	—	0.81	158	2.65
3.4	8.93	—	—	0.84	128.6	2.62
3.6	28.96	—	—	1.08	232.6	2.48
3.8	10.95	—	—	0.85	246.4	2.01
4.0	8.02	0.84	43.56	2.49	328.4	0.12
4.2	4.09	1.41	7.96	15.67	112.1	0.048
LLT0 1st discharge cycle						
4.2	3.76	1.31	8.33	12.41	64.44	0.058
4.0	5.65	1.14	11.05	8.54	72.34	0.047
3.8	4.72	0.81	22.89	3.88	80.19	0.068
3.6	5.95	0.78	30.16	3.48	116.2	0.13
3.4	5.26	0.75	31.59	2.77	155.6	0.74
3.2	7.99	—	—	0.80	163.4	1.92
3.0	8.04	—	—	0.78	166.9	2.06
LLT01 1st charge cycle						
3.0 (OCV)	4.64	—	—	1.24	37.69	4.77
3.2	4.49	—	—	1.21	25.56	5.03
3.4	4.19	—	—	1.20	26.67	5.04
3.6	3.89	—	—	1.17	26.64	4.96
3.8	4.92	—	—	1.21	34.28	4.30
4.0	3.70	1.50	21.30	7.24	60.91	0.046
4.2	7.26	149.5	22.84	1.82	25.63	0.081
LLT01 1st discharge cycle						
4.2	35.2	230	21.82	2.25	27.94	0.11
4.0	3.75	1.26	18.89	12.1	31.5	0.073
3.8	5.57	—	—	1.29	94.09	0.13
3.6	5.94	—	—	1.20	122.8	0.20
3.4	6.42	—	—	1.01	102.3	3.16
3.2	6.72	—	—	1.02	119.9	2.81
3.0	6.38	—	—	0.96	101	4.27

The Four-Point probe measurement data are showed in Table S3. As can be seen in Table S3, the electronic conductivity of pure LLTO (1.23×10^{-3} S cm^{-1}) is far more than that of other samples. With increasing of LLTO coating content, the electronic conductivity is increasing constantly.

Table S3. The Four-Point probe measurement data of LLTO, LLT0, LLT01, LLT03 and LLT05.

Sample	Resistivity (KΩ· cm)	Electronic conductivity (S cm^{-1})
LLTO	0.81	1.23×10^{-3}
LLT0	22.15	4.51×10^{-5}
LLT01	16.04	6.23×10^{-5}
LLT03	13.28	7.53×10^{-5}
LLT05	11.90	8.41×10^{-5}

[1] C. Ho, I. Raistrick, R. Huggins, Application of A-C Techniques to the Study of Lithium Diffusion in Tungsten Trioxide Thin Films, J. Electrochem. Soc. 127 (1980) 343

[2] W. Liu, J. Liu, K. Chen, S. Ji, Y. Wan, Y. Zhou, D. Xue, P. Hodgson, Y. Li, Enhancing the Electrochemical Performance of the $LiMn_2O_4$ Hollow Microsphere Cathode with a $LiNi_{0.5}Mn_{1.5}O_4$ Coated Layer, Chem. Eur. J. 20 (2014) 824

[3] S. Hu, Yu Li, J. Yin, H. Wang, X. Yuan, Q. Li, Effect of different binders on electrochemical properties of $LiFePO_4$/C cathode material in lithium ion batteries, Chem. Eng. J. 237 (2014) 497